Available online at www.sciencedirect.com
ScienceDirect
Journal of Magnetic Resonance 190 (2008) 339–345
JMR Journal of Magnetic Resonance
www.elsevier.com/locate/jmr

Communication

Resolution and sensitivity aspects of ultrafast *J*-resolved 2D NMR spectra

Patrick Giraudeau *, Serge Akoka

Université de Nantes, Nantes Atlantique Universités, CNRS, Laboratoire d'Analyse Isotopique et Electrochimique de Métabolismes, UMR 6006, B.P. 92208, 2 rue de la Houssinière, F-44322 Nantes Cedex 03, France

Received 22 October 2007; revised 27 November 2007
Available online 4 December 2007

Abstract

Recent ultrafast techniques enable *n*D NMR spectra to be obtained in a single scan. However, resolution enhancement in the ultrafast domain leads to important sensitivity losses and lineshape distortions. In order to understand better resolution and spatial encoding aspects of continuous phase-encoding schemes, a theoretical and experimental comparison of different excitation patterns is carried out. Molecular diffusion appears to be the main cause of signal-to-noise ratio decrease, and a multi-echo excitation scheme is proposed to limit its effects when a good resolution is needed. Results obtained on 2D *J*-resolved spectra are presented.

Keywords: Ultrafast 2D NMR; *J*-resolved spectroscopy; Resolution enhancement; Signal-to-noise ratio; Molecular diffusion

1. Introduction

The introduction of two-dimensional (2D) spectroscopy [1,2] is one of the most significant advances in the evolution of nuclear magnetic resonance (NMR) techniques. 2D NMR is used in a wide range of applications, from the study of chemical structures and dynamics to pharmaceutical and medical applications. However, it suffers from long acquisition times due to the necessary collection of numerous t_1 increments to obtain spectra with a good resolution.

Recently, a method based on ultrafast imaging techniques was proposed by Frydman and co-workers [3,4], enabling the acquisition of 2D NMR spectra within a single scan. In this so-called "ultrafast 2D NMR" technique, the usual t_1 encoding is replaced by a spatial encoding, which is decoded during a detection period by an echo planar imaging (EPI) scheme [5]. However, the discrete encoding mode initially proposed suffers from practical drawbacks as it requires fast gradient switching carefully synchronized with RF irradiation. Moreover, it leads to the appearance of undesirable "ghost peaks" in the indirect domain [6]. To deal with these limitations, a continuous encoding scheme was proposed by Shrot et al. [7], using a pair of continuously frequency-swept pulses applied during a bipolar gradient. Unfortunately, this method involves an amplitude modulation which is incompatible with phase-modulated techniques such as COSY [1] or *J*-resolved spectroscopy [8]. Different alternatives were then proposed [9–11] to obtain a phase-modulated encoding in order to circumvent these limitations.

Based on these continuous phase-modulated excitation schemes, we have recently proposed [12] a modification of the acquisition scheme to obtain *J*-resolved spectra where coupling constants are encoded along the direct v_2 domain. This scheme was coupled to both Pelupessy's [11] and Tal's [9] excitation patterns. In this study, it appeared that the resolution along the k/v_1 axis was quite disappointing compared to conventional 2D spectra. Moreover, resolution seemed to depend on the excitation scheme and it appeared impossible to improve it without a dramatic decrease of the signal-to-noise ratio.

* Corresponding author. Fax: +33 (0)2 51 12 57 12.
E-mail address: patrick.giraudeau@univ-nantes.fr (P. Giraudeau).

1090-7807/$ - see front matter © 2007 Elsevier Inc. All rights reserved.
doi:10.1016/j.jmr.2007.11.019

In the present paper, the approach of resolution and spatial encoding is rationalized in order to compare the different excitation schemes under similar conditions. An improvement of spatial encoding based on multiple-echoes is proposed, which allows increasing resolution while limiting signal-to-noise losses due to molecular diffusion effects. Results are applied to *J*-resolved spectroscopy.

2. Results and discussion

2.1. Comparison of different continuous phase-encoding schemes

The excitation scheme proposed by Pelupessy [11] and applied to *J*-resolved spectroscopy [12] is described in Fig. 1a. It starts with a 90° non-selective pulse, followed by a 180° chirp pulse of duration D^π with a linear frequency ramp applied during a magnetic field gradient $+G_e^\pi$. It is followed by an identical pulse applied during an inverted gradient $-G_e^\pi$. At the end of the first 180° pulse, it can be shown that the phase evolution of the system possesses constant, linear and quadratic terms, according to:

$$\phi_\pi = -\frac{D^\pi \Omega_1^2}{\gamma_e G_e^\pi L} - \frac{\gamma_e G_e^\pi L D^\pi}{4} - \frac{2D^\pi \Omega_1 z}{L} - \frac{D^\pi \gamma_e G_e^\pi z^2}{L} \quad (1)$$

where L is the excited height of the sample. In this expression we suppose that the frequency range of the chirp pulse is approximately adjusted to the one induced by the gradient, $\gamma_e G_e^\pi L$. The quadratic term prevents the formation of echo peaks in the indirect domain; however it is cancelled by the second 180° pulse, as well as the constant term. At the end of the excitation scheme, the phase evolution is given by

$$\phi_P^0 = \frac{4D^\pi \Omega_1 z}{L} \quad (2)$$

which possesses the linear dependence in $\Omega_1 \cdot z$ required by ultrafast 2D NMR. There is no constant term in Eq. (2); one could then expect that a spoiler prior to acquisition is not necessary. However, the application of a short gradient can be useful to compensate for experimental errors or to set the echoes at the desired position.

Tal et al. [9] proposed another method leading to a continuous phase encoding, described in Fig. 1b. It consists of a 90° continuous excitation performed by a chirp pulse of duration $D^{\pi/2}$ with a linear frequency ramp, applied during a positive gradient $G_e^{\pi/2}$. This excitation is immediately followed by a 180° chirp pulse of duration D^π, applied during a positive magnetic field gradient G_e^π. At the end of the 90° pulse, the phase evolution is given by

$$\phi^{\pi/2} = \frac{D^{\pi/2}}{2}\left(\Omega_1 - \frac{\Omega_1^2}{\gamma_e G_e^{\pi/2} L} - \frac{\gamma_e G_e^{\pi/2} L}{4}\right) + \frac{D^{\pi/2}}{L}\left[\frac{\gamma_e G_e^{\pi/2} L}{2} - \Omega_1\right] z - \frac{\gamma_e G_e^{\pi/2} D^{\pi/2}}{2L} z^2 \quad (3)$$

The quadratic term is removed by the 180° pulse when the condition

$$D^{\pi/2} G_e^{\pi/2} = 2D^\pi G_e^\pi \quad (4)$$

is respected [9]. Under this condition, the z-dependence of the phase evolution at the end of the encoding process can be written:

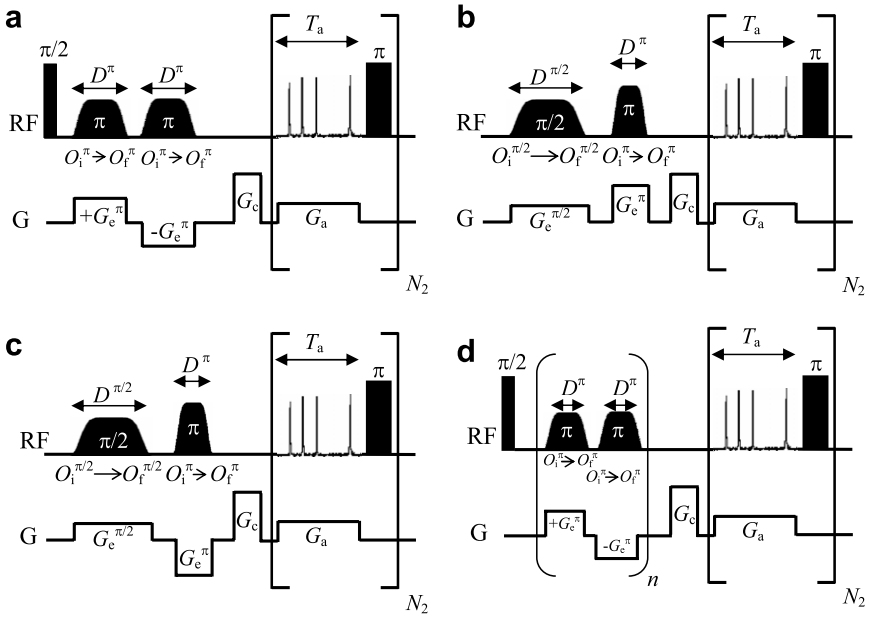

Fig. 1. Pulse sequences for the acquisition of ultrafast 2D *J*-resolved spectra, using phase-modulated encoding schemes proposed by Pelupessy (a) and Tal et al. (b), or using Tal's scheme with inverted G_e^π gradient (c). (d) Multiple-echo excitation scheme designed to limit diffusion effects. The G_c gradient prior to acquisition is adjusted to set the middle of the chemical shift range in the middle of the detection period T_a. The 180° pulse phase is alternated $(y, y, -y, -y)$ to avoid undesirable stimulated echoes.

$$\phi_T^0(z) = \left[-\frac{D^{\pi/2}\gamma_e G_e^{\pi/2}}{2} + \frac{D^{\pi/2}}{L}\left(1 - \frac{G_e^{\pi/2}}{G_e^{\pi}}\right)\Omega_1 \right] \cdot z \quad (5)$$

assuming that the frequency range of each chirp pulse matches the one of the corresponding gradient. In Eq. (5), the Ω_1-independent contribution is an offset that can be easily compensated by an appropriate gradient G_c prior to acquisition. The evolution phase also contains a z-independent term which leads to a first-order phase distortion. Spectra are represented in magnitude mode to avoid dealing with this distortion.

A slightly different version of Tal's encoding pattern was suggested by Andersen and Kockenberger [10]. Here, the gradient G_e^{π} applied during the 180° pulse is inverted (Fig. 1c). When calculating the phase $\phi_{Ti}^0(z)$ at the end of such a scheme, we obtain the following expression:

$$\begin{aligned}\phi_{Ti}^0 = &\left[-D^{\pi}\left(\frac{\Omega_1^2}{\gamma_e G_e^{\pi} L} + \frac{\gamma_e G_e^{\pi} L}{4}\right) \right.\\ &\left. -\frac{D^{\pi/2}}{2}\left(\Omega_1 - \frac{\Omega_1^2}{\gamma_e G_e^{\pi/2} L} - \frac{\gamma_e G_e^{\pi/2} L}{4}\right)\right]\\ &+\left[-\frac{D^{\pi/2}\gamma_e G_e^{\pi/2}}{2} + (D^{\pi/2} + 2D^{\pi})\frac{\Omega_1}{L}\right]\cdot z\\ &+\gamma_e\left[\frac{D^{\pi/2}G_e^{\pi/2} - 2D^{\pi}G_e^{\pi}}{2L}\right]\cdot z^2 \end{aligned} \quad (6)$$

When condition (4) is fulfilled, the quadratic term is cancelled and the z-dependence of the phase evolution at the end of the encoding process can be written:

$$\phi_{Ti}^0(z) = \left[-\frac{D^{\pi/2}\gamma_e G_e^{\pi/2}}{2} + \frac{D^{\pi/2}}{L}\left(1 + \frac{G_e^{\pi/2}}{G_e^{\pi}}\right)\Omega_1 \right] \cdot z \quad (7)$$

The evolution phase also contains a z-independent term which leads to a first-order phase distortion that can be eliminated using magnitude mode. Contrary to Andersen and Kockenberger's recommendation [10], it appears that the sweep direction of the 180° pulse should not be reversed, as the quadratic term could not be cancelled in this case. Eq. (7) is very similar to Eq. (5), except that factor $(1 - G_e^{\pi/2}/G_e^{\pi})$ is replaced by $(1 + G_e^{\pi/2}/G_e^{\pi})$.

At this stage, it appears necessary to define parameters that would help us to compare the three excitation schemes under the same conditions. To perform this comparison, we shall call T_e the average time spent by the magnetization in the transverse plane. The value of T_e for each encoding scheme is given in Table 1. Encoding schemes should be compared with identical T_e values to make sure they have the same dependence on transverse relaxation. We will also compare the spatio-temporal encoding constants C, which is the $\Omega_1 \cdot z$ dependence of the phase evolution at the end of the encoding process [3]. For each scheme, C is expressed as a function of T_e and the resulting expression is given in Table 1.

It clearly appears that for identical T_e values, the spatial encoding level is higher with Pelupessy's excitation scheme than with Tal's, because the latter is modulated by the $G_e^{\pi/2}/G_e^{\pi}$ ratio. However, Tal's scheme with inverted G_e^{π} gradient leads to the same encoding constant than Pelupessy's, as it does not depend any more on the gradient ratio for a given T_e value.

Table 1
Relevant parameters (average time in transverse plane T_e and spatio-temporal encoding level C) for different continuous encoding schemes

Encoding scheme	T_e	C
Pelupessy	$2D^{\pi}$	$\frac{2T_e}{L}$
Tal	$\frac{D^{\pi/2}}{2} + D^{\pi}$	$\frac{2T_e}{L}\cdot\frac{1-G_e^{\pi/2}/G_e^{\pi}}{1+G_e^{\pi/2}/G_e^{\pi}}$
Tal with inverted G_e^{π} gradient	$\frac{D^{\pi/2}}{2} + D^{\pi}$	$\frac{2T_e}{L}$

The frequency range for each WURST pulse is supposed to match approximately the one induced by the corresponding gradient and for the two last schemes, condition (4) is supposed to be fulfilled.

It is also interesting to compare the resolution of the different methods, which can be evaluated by the half-height width $\delta v^{1/2}$ in the ultrafast k/v_1 dimension. $\delta v^{1/2}$ can be calculated by Eq. (8):

$$\delta v^{1/2} = \frac{\delta\tau^{1/2}}{\Delta\tau_a}\cdot\Delta v \quad (8)$$

In this expression, $\Delta\tau_a$ is the time between two echoes detected by the same acquisition gradient, corresponding to two peaks separated by Δv; $\delta\tau^{1/2}$ is the temporal half-height width of the echo peaks. To calculate this expression for a given encoding scheme, it should be reminded that the echo appears at the exact moment τ_a when the dephasing induced by the acquisition gradient, $\gamma_a G_a \tau_a z$, compensates for the z-dependent term of the phase at the beginning of the detection gradient, $\phi^0(z)$ [3]. Thus, the echo temporal position in the ultrafast dimension is given by Eq. (9):

$$\tau_a = \frac{\phi^0(z)}{\gamma_a G_a z} = \frac{C\Omega}{\gamma_a G_a} \quad (9)$$

and the duration $\Delta\tau_a$ separating two echoes can be calculated by:

$$\Delta\tau_a = \frac{C}{\gamma_a G_a}\cdot 2\pi\Delta v \quad (10)$$

Moreover, if the lineshape is approximated to a Sine function [13], the temporal half-height width $\delta\tau^{1/2}$ is approximately $7.58/(\gamma_a G_a L)$. Finally, it can be shown that $\delta v^{1/2}$ is inversely proportional to the spatio-temporal encoding constant C according to:

$$\delta v^{1/2} \approx \frac{1.21}{LC} \quad (11)$$

Eq. (11) shows that C is sufficient to characterize resolution. The higher C is, the better resolution is. The C values obtained for both encoding schemes (Table 1) demonstrate that the highest resolution is obtained for Pelupessy's scheme and for Tal's scheme with inverted G_e^{π} gradient.

As a conclusion, Tal's scheme using inverted gradient should theoretically lead to the same result as Pelupessy's

scheme. To check this assessment, we performed *J*-resolved ultrafast experiments using both excitation schemes with the same T_e (60 ms) and same gradient amplitudes. For Tal's inverted scheme, the $G_e^{\pi/2}/G_e^{\pi}$ ratio was initially set to 1. The spectra obtained on a 3-ethyl bromopropionate sample are presented in Fig. 2. As expected, both spectra almost have the same resolution in the ultrafast dimension. The half-height width, measured on the 2D ultrafast spectrum projection along k/v_1 axis, is 17 ± 1 Hz for Pelupessy's scheme (Fig. 2a) and 20 ± 1 Hz for Tal's inverted scheme (Fig. 2b). We also varied the $G_e^{\pi/2}/G_e^{\pi}$ ratio for Tal's inverted scheme and we do not observe significant differences for half-height widths, which confirms that the resolution does not depend on the gradient ratio. However, in these experiments, measured $\delta\nu^{1/2}$ values are higher than the ones predicted by Eq. (11) (10 Hz for $T_e = 60$ ms), which may be due to experimental parameter variations.

In spite of similar resolutions for both schemes, the signal-to-noise ratio is higher for Pelupessy's excitation scheme ($S/N = 140 \pm 15$, measured on the highest peak of the quadruplet) than for Tal's ($S/N = 70 \pm 30$). Moreover, the peak intensities on the projection seem more distorted for Tal's scheme (Fig. 2b). The three peaks at 2.9, 3.6 and 4.2 ppm are expected to have the same intensities as they each correspond to two protons, which is clearly not the case here. However, it should be noted that the time T_e spent by magnetizations in the transverse plane is an average value for Tal's scheme whereas it is an exact value for Pelupessy's, as in the second case all magnetizations are flipped in xy plane at the same time.

Because of these intensity distortions, we were not able to use the same cross-section levels in Fig. 2a and b in order to obtain a correct definition of the weakest multiplets. This explains why 2D peaks look different in Fig. 2 in spite of similar resolutions.

It should also be noted that Tal's scheme appears much more difficult to set than Pelupessy's, because the 90° pulse must be carefully calibrated to obtain an accurate $\pi/2$ excitation with an adiabaticity parameter of 0.068 [14], and also because the G_e^{π} value must be adjusted to obtain the sharpest echo peaks, as noticed by Tal et al. [9]. Consequently, Pelupessy's scheme appears easier to implement in routine procedures.

2.2. Resolution versus sensitivity

According to the results presented in Table 1, resolution could be improved by simply increasing the value of T_e. To verify this assessment, we increased the duration of the excitation period ($T_e = 120$ ms) for Pelupessy's excitation scheme [11], by doubling the duration of the 180° excitation pulses, which should theoretically lead to $\delta\nu^{1/2} = 5$ Hz, according to Eq. (11). The corresponding spectrum is shown in Fig. 3a. The expected resolution improvement is observed (half-height width decreased to 13 ± 1 Hz) even though $\delta\nu^{1/2}$ is higher than the expected value. However, the signal-to-noise ratio dramatically decreases ($S/N = 15 \pm 5$ for the highest peak of the quadruplet). Moreover, the projection shows important lineshape distortions, particularly for the triplet at 1.3 ppm. This is probably due to an incomplete refocusing of corresponding magnetizations. T_e was also increased to 120 ms for Tal's scheme and the same evolution was observed. Sensitivity decrease was too important to be able to measure S/N ratio and resolution.

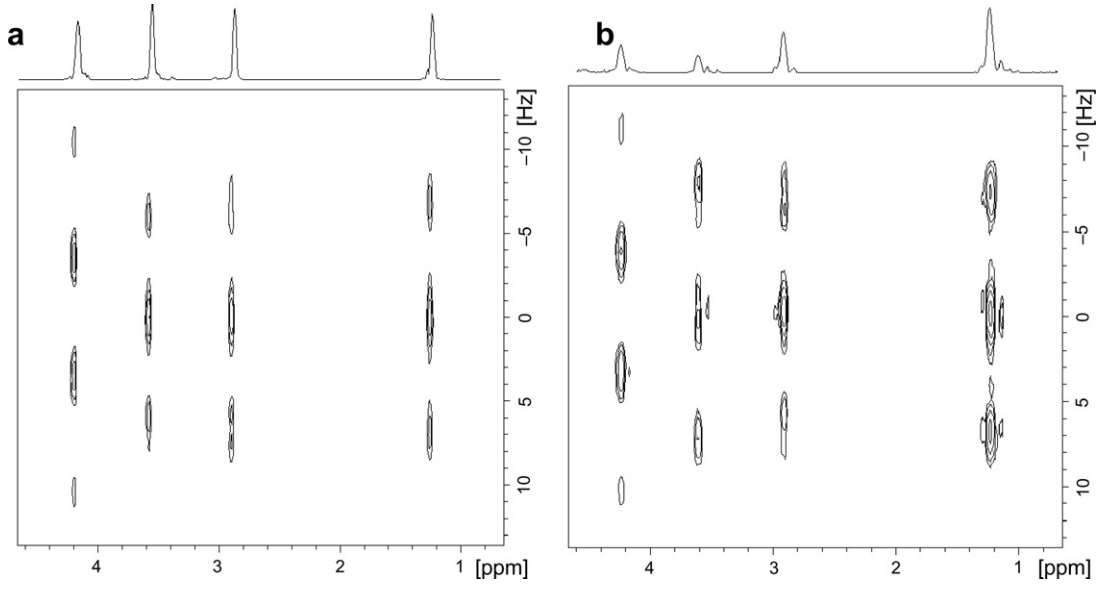

Fig. 2. Comparison between ultrafast 500 MHz *J*-resolved spectra acquired on a 100 mmol l^{-1} 3-ethyl bromopropionate sample in $CDCl_3$ at 298 K. Both spectra were obtained in 500 ms, with the same average excitation time $T_e = 60$ ms. Spectra obtained with Pelupessy's encoding scheme (a) or Tal's encoding scheme using inverted G_e^{π} gradient (b). Both spectra were processed with the same apodization function and post processing parameters, as described in Section 4.

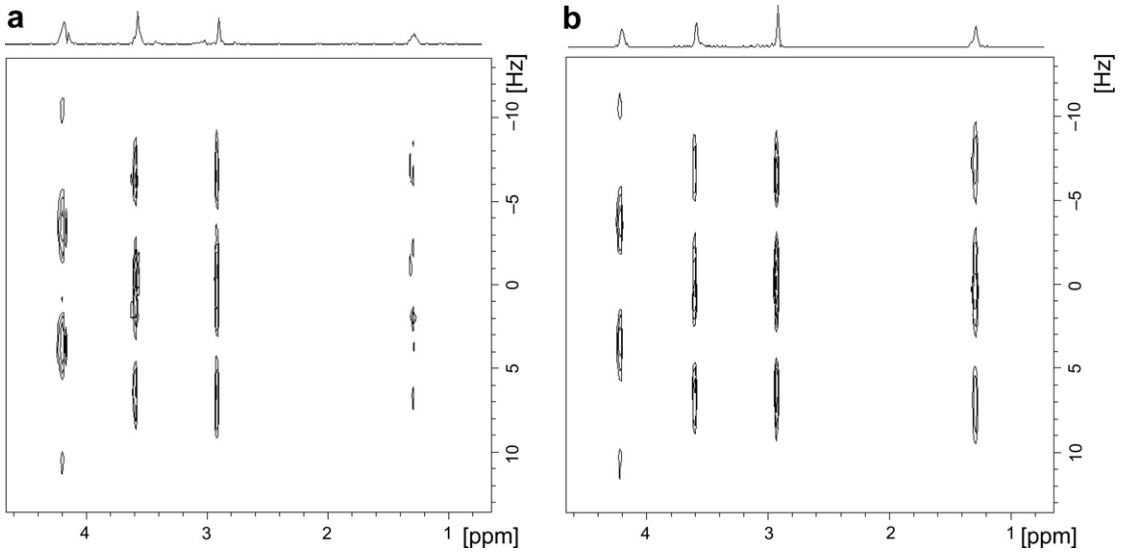

Fig. 3. 500 MHz ultrafast *J*-resolved spectra obtained acquired on a 100 mmol l^{-1} 3-ethyl bromopropionate sample in $CDCl_3$ at 298 K. Both spectra were obtained in 500 ms, with the same average excitation time $T_e = 120$ ms. (a) Spectrum obtained with Pelupessy's encoding scheme consisting of two 60 ms 180° pulses. (b) Spectrum obtained with multi-echo excitation scheme formed by six 20 ms 180° pulses. Both spectra were processed with the same apodization function and post processing parameters, as described in Section 4.

The aforementioned effects may be due to molecular diffusion or transverse relaxation. However, we measured the transverse relaxation times of 3-ethyl bromopropionate and values between 0.4 and 1.5 s were obtained, which is much higher than the duration of the excitation period. The maximum magnetization decrease at the end of the 120 ms excitation period is only 26% for $T_2 = 0.4$ s, which clearly indicates that transverse relaxation is not the main cause of sensitivity decrease. Moreover, the same spectrum was obtained in a more viscous solvent (DMSO-d_6) in order to limit diffusion effects. The S/N ratio was increased by a factor of 2, which confirms that diffusion is the main reason that could explain the S/N ratio decrease previously described. In spite of the good results obtained in DMSO-d_6, we chose to keep using $CDCl_3$ as a solvent for the continuation of our study, as in practice it is not always possible to choose a viscous solvent.

To evaluate the effect of diffusion for another pulse sequence, we also performed ultrafast TOCSY experiments on 3-ethyl bromopropionate in $CDCl_3$, with $T_e = 60$ and 120 ms. S/N for cross-peaks was decreased from 23 ± 1 to 16 ± 2, which shows that diffusion effects occur even when a mixing period is present. A more general, theoretical and quantitative analysis of diffusion losses will be given in an ulterior paper.

J-resolved experiments performed with different excitation gradient amplitudes showed important S/N decrease when increasing G_e^{π} values, which also confirms the influence of molecular diffusion. Consequently, the first possibility to limit diffusion effects in pulse sequences with long T_e values is to use weaker gradient amplitudes. However, all the spectra presented above were already obtained with the smallest amplitudes available on our spectrometer, as they were only 2% of their maximum strength. Lower values would lead to important signal distorsions. As a consequence, it appears necessary to propose an excitation scheme designed to limit diffusion effects when a high T_e is required to obtain a good resolution. To achieve this, we propose a multi-echo encoding pattern which is described in Fig. 1d. In this pulse sequence based on Pelupessy's technique [11], the two 180° chirp pulses are replaced by a succession of shorter 180° pulses pairs applied during alternated gradients. The duration of 180° pulses is given by $T_e/(2n)$, where $2n$ is the number of echoes. For identical T_e values, theoretical spatial encoding level and resolution are the same as in Pelupessy's scheme, but diffusion effects should be reduced because shorter gradients are employed [15,16].

The application of this multi-echo pattern is presented in Fig. 3b, for a 6 echo scheme with 20 ms pulses, leading to a total T_e of 120 ms. The resolution is the same ($\Delta\nu^{1/2} = 13 \pm 1$ Hz) as for Pelupessy's pulse sequence with $T_e = 120$ ms (Fig. 3a). Moreover, sensitivity has been increased by a factor of 2 ($S/N = 30 \pm 8$ for the highest peak of the quadruplet) and all peaks are now well defined. This shows the efficiency of multi-echo excitation to limit diffusion effects.

In order to further improve sensitivity, we tried to use more than 6 echoes while keeping T_e unchanged. However, it did neither increase nor decrease S/N ratio. Moreover, experiments performed at different T_e values showed that multi-echo excitation leads to sensitivity and resolution losses when T_e is too small, i.e. when diffusion is not predominant. This unexpected negative effect could be due to adiabaticity losses when 180° pulse durations become shorter, since the adiabaticity factor is directly proportional to the pulse duration [17]. These observations underline the limits of the multi-echo method that should be

applied with care. In order to choose the experimental parameters for a given excitation scheme, the minimum adiabaticity factor reached during the pulse could be calculated according to [17].

Finally, as suggested in [12], we also tried to combine Tal's and Pelupessy's excitation schemes, however resolution and S/N improvements were less significant than the ones obtained by multi-echo excitation pattern based on Pelupessy's scheme.

3. Conclusion

The comparison between different continuous encoding schemes leads to the conclusion that Tal's encoding scheme with inverted gradient is as efficient as Pelupessy's concerning resolution aspects. Based on Pelupessy's technique, the new multi-echo encoding scheme presented above offers the possibility of acquiring 2D ultrafast spectra with good resolution while limiting sensitivity losses due to molecular diffusion. It is applied to *J*-resolved spectroscopy but might be useful for other single-scan *n*D experiments.

As a conclusion, we may define the best conditions for acquiring high-resolution ultrafast 2D spectra: high T_e value compensated by multi-echo excitation, small gradient amplitudes and viscous solvent when it is possible. The temperature effects should also be taken into consideration.

Another important aspect of ultrafast *J*-resolved spectroscopy is the influence of homonuclear *J*-couplings on peak intensities, which was not considered in this work. A detailed analysis of this aspect will be given elsewhere.

Resolution improvements of ultrafast spectra could progressively lead to the replacement of conventional techniques by ultrafast methods in a wide range of applications, from structural analysis to *in vivo* spectroscopy. The use of such techniques for quantitative analysis [18] will be considered in later works. However, it should be kept in mind that in spite of the improvements presented here, ultrafast acquisition can be used only when sufficient S/N is available [19], which could be a problem at low concentrations.

4. Experimental

In order to obtain a 100 mmol l^{-1} solution, 13.0 μl of 3-ethyl bromopropionate, purchased from Sigma Aldrich, were dissolved in 1 ml of $CDCl_3$ or 1 ml of DMSO-d_6. After homogenization, each sample was filtered and analysed in a 5 mm tube.

NMR spectra were recorded at 298 K on a Bruker Avance 500 DRX spectrometer, at a frequency of 500.13 MHz with a triple resonance TBI probe including *z*-axis gradient.

Ultrafast 2D *J*-resolved spectra were obtained with ± 1.1 G cm^{-1} excitation gradients and Wurst-8 pulses [20] with a sweep range of 9.4 kHz. For Tal's inverted scheme, the $\pi/2$ pulse, applied for 60 ms, was carefully calibrated to obtain an accurate 90° excitation with an adiabaticity parameter of 0.068 [14]. It was followed by a π Wurst-8 adiabatic pulse applied for 30 ms. For Pelupessy's encoding scheme, Wurst-8 adiabatic pulses [20] were applied for 30 ms for $T_e = 60$ ms, or for 60 ms for $T_e = 120$ ms. The same pulses were used for multi-echo encoding, with durations depending on T_e and number of echoes.

The *J*-resolved detection block was formed of 64 detection gradients of duration $T_a = 6.9$ ms each and a strength G_a adapted to observe the relevant chemical shift range during T_a. For each experiment, the gradient G_c, applied during 500 μs, was set to adjust the centre of the chemical shift range in the middle of the acquisition window.

For TOCSY [21] spectra, the same excitation block as for *J*-resolved spectra was used, followed by a 80 ms DIPSI-2 [22] mixing period. The detection block was formed of 128 alternated detection gradients of duration $T_a = 280$ μs each with a strength G_a adapted to observe the relevant chemical shift range.

All spectra were processed in the same way: zero-filling once and shifted square sine-bell apodization functions in v_2 dimension. All ultrafast spectra were subjected to noise subtraction along the k/v_1 axis, but S/N and resolution measurements were performed before this operation.

All spectra were analysed using the Bruker program Topspin 2.0. The specific processing for ultrafast spectra was performed using our home-written routine in Topspin. S/N ratios and $\Delta v^{1/2}$ are average values determined on five successive experiments.

References

[1] W.P. Aue, E. Bartholdi, R.R. Ernst, Two-dimensional spectroscopy. Application to nuclear magnetic resonance, J. Chem. Phys. 64 (1976) 2229–2246.
[2] J. Jeener, Lecture presented at Ampere International Summer School II, Basko Polje, Yugoslavia, September 1971.
[3] L. Frydman, A. Lupulescu, T. Scherf, Principles and features of single-scan two-dimensional NMR spectroscopy, J. Am. Chem. Soc. 125 (2003) 9204–9217.
[4] L. Frydman, T. Scherf, A. Lupulescu, The acquisition of multidimensional NMR spectra within a single scan, Prod. Natl. Acad. Sci. USA 99 (2002) 15858–15862.
[5] P. Mansfield, Spatial mapping of the chemical shift in NMR, Magn. Reson. Med. 1 (1984) 370–386.
[6] Y. Shrot, L. Frydman, Ghost-peak suppression in ultrafast two-dimensional NMR spectroscopy, J. Magn. Reson. 164 (2003) 351–357.
[7] Y. Shrot, B. Shapira, L. Frydman, Ultrafast 2D NMR spectroscopy using a continuous spatial encoding of the spin interactions, J. Magn. Reson. 171 (2004) 163–170.
[8] W.P. Aue, J. Karhan, R.R. Ernst, Homonuclear broad band decoupling and two-dimensional *J*-resolved NMR spectroscopy, J. Chem. Phys. 64 (1976) 4226–4227.
[9] A. Tal, B. Shapira, L. Frydman, A continuous phase-modulated approach to spatial encoding in ultrafast 2D NMR spectroscopy, J. Magn. Reson. 176 (2005) 107–114.
[10] N.S. Andersen, W. Köckenberger, A simple approach for phase-modulated single-scan 2D NMR spectroscopy, Magn. Reson. Chem. 43 (2005) 791–794.
[11] P. Pelupessy, Adiabatic single scan two-dimensional NMR spectroscopy, J. Am. Chem. Soc. 125 (2003) 12345–12350.
[12] P. Giraudeau, S. Akoka, A new detection scheme for ultrafast *J*-resolved spectroscopy, J. Magn. Reson. 2007 (2007) 352–357.

[13] B. Shapira, A. Lupulescu, Y. Shrot, L. Frydman, Line shape considerations in ultrafast NMR, J. Magn. Reson. 166 (2004) 152–163.
[14] Y. Shrot, L. Frydman, Spatially encoded NMR and the acquisition of 2D magnetic resonance images within a single scan, J. Magn. Reson. 172 (2005) 179–190.
[15] B. Geil, Measurement of translational molecular diffusion using ultrahigh magnetic field gradient NMR, Concept Magn. Reson. 10 (1998) 299–321.
[16] H. Carr, E.M. Purcell, Effects of diffusion on free precession in nuclear magnetic resonance experiments, Phys. Rev. 94 (1954) 630.
[17] E. Tenailleau, S. Akoka, Adiabatic ^{1}H decoupling scheme for very accurate intensity measurements in ^{13}C NMR, J. Magn. Reson. 185 (2007) 50–58.
[18] P. Giraudeau, N. Guignard, H. Hillion, E. Baguet, S. Akoka, Optimization of homonuclear 2D NMR for fast quantitative analysis: application to tropine–nortropine mixtures, J. Pharmaceut. Biomed. Anal. 43 (2007) 1243–1248.
[19] L. Frydman, Single-scan multidimensional NMR, C. R. Chimie 9 (2006) 336–345.
[20] E. Kupce, R. Freeman, Adiabatic pulses for wideband inversion and broadband decoupling, J. Magn. Reson. A 115 (1995) 273–276.
[21] L. Braunschweiler, R.R. Ernst, Coherence transfer by isotropic mixing: application to proton correlation spectroscopy, J. Magn. Reson. 53 (1983) 521–528.
[22] A.J. Shaka, C.J. Lee, A. Pines, Iterative schemes for bilinear operators; application to spin decoupling, J. Magn. Reson. 77 (1988) 274–293.